VSB TECHNICAL UNIVERSITY OF OSTRAVA | FACULTY OF MECHANICAL ENGINEERING

**MM Science Journal | www.mmscience.eu**
ISSN 1803-1269 (Print) | ISSN 1805-0476 (On-line)
**Special Issue | TEAM 2024**
**Transdisciplinary and Emerging Approaches to Multidisciplinary Science**
**11.9.2024 – 13.9.2024, Ostrava, Czech Republic**
DOI: 10.17973/MMSJ.2024_12_2024127

MM SCIENCE JOURNAL

**TEAM2024-00040**

# GENETIC PROGRAMMING-BASED PREDICTIVE MODELLING OF MOISTURE RATIO IN DRYING OF GRAPES USING DESICCANT ROTARY DRYER

Krunal Mudafale[1], Kanak Kalita[1,2,*], S P Samal[3], Pradeep Jangir[4,5,6,7]

[1] Department of Mechanical Engineering, Vel Tech Rangarajan Dr, Sagunthala R&D Institute of Science and Technology, Avadi, 600062, India. vtd722@veltech.edu.in. drkanakkalita@veltech.edu.in.

[2] Jadara Research Center, Jadara University, Irbid 21110, Jordan.

[3] Department of Biosciences, Saveetha School of Engineering, Saveetha Institute of Medical and Technical Sciences, Chennai 602105, India. spsamal24@gmail.com.

[4] University Centre for Research and Development, Chandigarh University, Mohali 140413, India. pkjmtech@gmail.com.

[5] Applied Science Research Center, Applied Science Private University, Amman 11931, Jordan.

[6] Department of CSE, Graphic Era Hill University, Dehradun 248002, India.

[7] Department of CSE, Graphic Era Hill University, Graphic Era Deemed to Be University, Dehradun 248002, India.

*Corresponding author; e-mail: drkanakkalita@veltech.edu.in

**Abstract**
In this study predictive models are developed for moisture ratio in the drying process of grapes using a desiccant rotary dryer. Response Surface Methodology (RSM) and Genetic Programming (GP) are employed to capture the relationship between critical drying parameters—temperature, airflow velocity and time—and the moisture ratio. The RSM model demonstrated high accuracy with a correlation coefficient of 0.992, whereas the GP model achieved a slightly lower correlation coefficient of 0.983. However, GP offered a simpler and interpretable structure. Comparative analysis reveals that both the models are in close proximity of experimental data and thus, are suitable for predicting drying parameters in food processing. This study highlights the effectiveness of using GP to enhance efficiency in grape drying— with implications for broader food dehydration applications.

**Keywords:**
Modelling, drying, response surface, genetic programming, dryer

## 1 INTRODUCTION

Drying is a fundamental process in various industries, particularly in food processing, where it involves the thermal removal of moisture to produce a stable, solid product. The transfer of energy as heat to the wet solid occurs through mechanisms such as convection, conduction, radiation, or a combination thereof [Mujumdar 2020]. In the context of food preservation, drying plays a crucial role in extending the shelf life of agricultural products, maintaining their quality and preventing spoilage [Mercer 2023].

Dryers are essential devices in process technology, designed to remove solvents from solid powders using methods like convective, conductive, or radiative drying for effective thermal separation [Zhou 2022]. Among the various types of dryers, solar dryers have gained attention and are categorized into direct, indirect, mixed-mode and hybrid types [Gautam 2024]. Rotary dryers, in particular, are utilized to reduce moisture content in biomass. They feature a rotating drum that ensures uniform drying through controlled airflow and heat application [Nursani 2021].

The drying of grapes is a significant process in the production of raisins and other dehydrated grape products. Effective drying enhances shelf life, reduces waste and improves transportation efficiency. Key process parameters influencing the quality of dried grapes are temperature, humidity, airflow and drying time [Palacios-Rosas 2023]. Optimization of these parameters is crucial, as they directly affect the nutritional and sensory qualities of the final product [Homayoonfal 2023].

Several studies have explored various drying methods for grapes. For instance, Singh et al. [Singh 2023a] developed a novel photovoltaic-thermal and thermoelectric generator integrated solar dryer for grapes, achieving a reduction in moisture content from 4.00 to 1.71 (d.b.). Similarly, Kalavathidevi et al. [Kalavathidevi 2023] emphasized the use of solar-powered dryers to reduce moisture content.

Different pretreatment methods have also been investigated to improve drying efficiency and product quality. Ünal and Şener [Ünal 2023] studied the effects of sun-drying and treatments with potassium carbonate and ashy water on the antioxidant properties and physicochemical characteristics of raisins. Baslar and Karabulut [Baslar 2023] evaluated the drying kinetics of Sultana and Besni grapes, highlighting that the Page model effectively described the drying behavior and that temperature significantly impacted moisture diffusivity and drying efficiency.

Despite these advancements, there remains a gap in the literature regarding the application of advanced modelling

and optimization techniques in the drying process of grapes, particularly using desiccant rotary dryers. Modelling and optimization are critical for enhancing the efficiency and accuracy of drying processes. Without these techniques, drying processes may lack efficiency and accuracy, leading to suboptimal designs [Yang 2013]. Modelling enhances the understanding of complex systems, improves decision-making and facilitates better management of uncertainty in system design [Aughenbaugh 2004]. Furthermore, the application of mathematical models can lead to improved performance, cost reduction and enhanced overall management of information systems [Lvovich 2019] [Veeranan 2016]. Recent research indicates a growing interest in modelling and optimization techniques, particularly using response surface methodology (RSM) and machine learning (ML) methods to enhance drying processes and energy efficiency in food dehydration [Kilic 2023] [Chen 2023]. While the RSM-based models can be easily visualized as parametric equations, the same is not true for ML models. Most ML models operate as black box models and thus, it is in not convenient to develop parametric equations. To bridge this gap, a genetic programming (GP)-based modelling approach is adopted in this study. GP models are tuned over several iterations from a training data and are visualized as parametric equations. Further by controlling the inputted functions, terminals and the hyperparameters like depth of tree, the complexity and compactness of the model can be adjusted.

The present study aims to fill this gap by developing a GP-based model to predict the moisture ratio during the drying of grapes in a desiccant rotary dryer. To ascertain the utility and effectiveness of the developed GP model, it is compared with a RSM model. By integrating advanced modelling and optimization techniques, this research seeks to enhance the drying process of grapes.

The rest of the paper is organized as follows— Section 2 details the experimental setup and the methods used to model and optimize the grape drying process. Section 3 details the results and critically discusses them. Section 4 summarizes the major findings of the work and presents some future directions.

## 2 METHODOLOGY

The methodology followed in this paper is shown in Figure 1. The process parameters are chosen based on literature review. Based on the experimental design, as discussed in Section 2.2, 15 experiments are carried out in an in-house developed desiccant rotary dryer. The design and working of the desiccant rotary dryer are discussed in Section 2.1. Next, parametric equations are developed to express the moisture ratio as a function of the considered process parameters. This is done using RSM and GP methods as discussed in Section 2.3 and 2.4, respectively.

### 2.1 Experimental Setup

The experimental setup, illustrated in Figure 2, consists of three main sections— the inlet section, the drying chamber and the silica gel bed section. In the inlet section (Point 4), a 0.5 HP DC motor powers a convergent fan system that draws ambient air into the dryer. This air is propelled toward a heating coil (Point 14), where it is heated through conduction, convection and radiation heat transfer mechanisms. A hotwire anemometer located at Point 4 measures the air velocity entering the system. Thermocouples placed at Points 13, 14, 15 and 16 monitor temperatures within the dryer to ensure optimal operating conditions.

After heating, the air passes through the silica gel bed section (Point 6). Here, 500 grams of silica gel removes moisture from the air, producing warm, dry air suitable for efficient drying. The dehumidified air then enters the drying chamber (Point 5), which contains perforated trays mounted on a rotating mechanism (Figure 3). This mechanism is driven by a 0.25 horsepower (HP) motor and is constructed from mild steel (layered with aluminum foil) with dimensions of 23 × 23 inches. As the trays rotate, the warm, dry air uniformly contacts the materials, enhancing moisture evaporation through combined conductive, convective and radiative heat transfer. The specification of the various components is presented in Table 1.

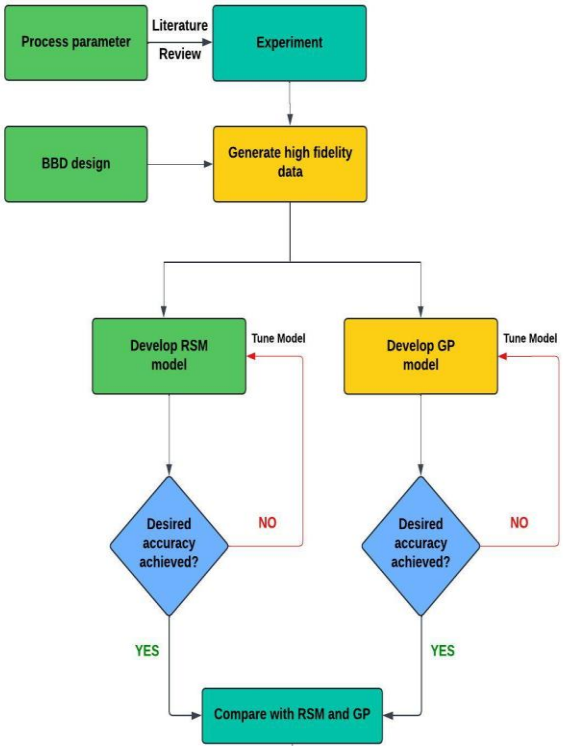


*Fig. 1: Flowchart of the proposed methodology*

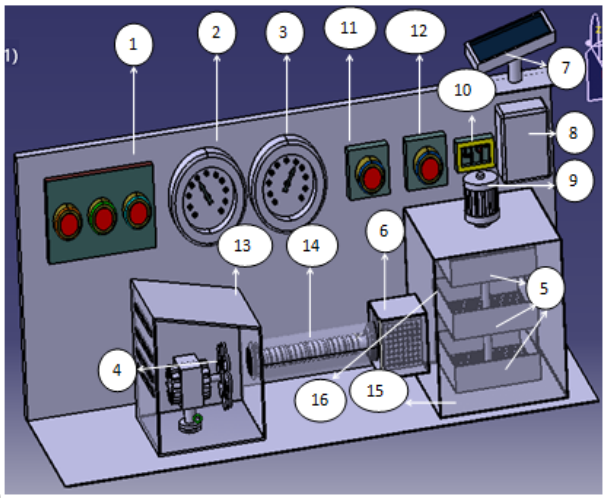


| | |
|---|---|
| 1. Control Switches | 2. Voltmeter |
| 3. Ammeter | 4. Exhaust DC Fan |
| 5. Perforated Tray | 6. Silica Gel Bed |
| 7. Solar Panel | 8. Battery |
| 9. 0.25Hp Motor | 10. Digital Temperature Indicator |
| 11. Dimmer stat | 12. Fan Regulator |
| 13. Inlet Duct Temperature | 14. Heater Temperature |
| 15. Chamber Temperature | 16. Chamber Temperature |

*Fig. 2: CAD model of experimental setup*

### 2.2 Design of Experiments

The experimental design was structured using the Box-Behnken Design (BBD). Three critical independent variables were selected based on their influence on the drying process— drying temperature ($T$), air velocity ($V$) and drying time ($t$). Each variable was studied at three levels—low, medium and high—to capture a wide range of operating conditions. The specific levels for each factor were determined based on preliminary trials and literature recommendations, ensuring practical relevance and feasibility. The BBD design used in this study is shown in Table 2.

The choice of BBD over other designs was motivated by its rotatability and efficiency in requiring fewer experimental runs than a central composite design, without sacrificing the ability to fit a second-order polynomial model. The design matrix generated by BBD included 15 experimental runs, encompassing combinations of the three factors at different levels while avoiding extreme combinations that could be impractical or unsafe.

The dependent variable measured in each experiment was the moisture ratio ($MR$) of the grapes, calculated using,

$$MR = \frac{M_t - M_e}{M_0 - M_e} \quad (1)$$

where $M_t$ is the moisture content at time t, $M_0$ is the initial moisture content and $M_e$ is the equilibrium moisture content. The experiments were randomized to minimize the effects of uncontrolled variables and were conducted in triplicate to ensure reproducibility and reliability of the data.

*Tab. 1: Specification of various components*

| Component | Material | Specifications |
|---|---|---|
| Duct arrangement | Mild Steel | 12 × 12 inch |
| Inlet fan | Fiber | 8 × 8 inch |
| Heater | Ceramic base with aluminum wire heating coil | 1500 watt |
| Desiccant chamber | 5 tray of aluminum beds loaded with silica gel | 500 gm |
| Drying chamber | 3 trays of mild steel layered with aluminum foil | 23 × 23 inch |
| Rotatory Mechanism of drying chamber | Motor | 12 × 12 inch |

*Tab. 2: BBD-based experimental $MR$ and predictions by RSM and GP*

| Drying Temperature, $T$ ($°C$) | Drying Time, $t$ ($min$) | Air Flow Rate, $V$ ($m/s$) | Moisture Ratio, $MR$ | RSM | GP |
|---|---|---|---|---|---|
| 50 | 3000 | 1 | 0.329239 | 0.3309 | 0.3038325 |
| 65 | 3000 | 1 | 0.343771 | 0.344 | 0.31760925 |
| 50 | 4200 | 1 | 0.323993 | 0.3303 | 0.3038325 |
| 65 | 4200 | 1 | 0.342149 | 0.3433 | 0.31760925 |
| 50 | 3600 | 0.5 | 0.297674 | 0.2989 | 0.2712075 |
| 65 | 3600 | 0.5 | 0.311597 | 0.312 | 0.28498425 |
| 50 | 3600 | 1.5 | 0.374938 | 0.3706 | 0.3364575 |
| 65 | 3600 | 1.5 | 0.380645 | 0.3836 | 0.35023425 |
| 57.5 | 3000 | 0.5 | 0.308813 | 0.3071 | 0.278095875 |
| 57.5 | 4200 | 0.5 | 0.299996 | 0.2955 | 0.278095875 |
| 57.5 | 3000 | 1.5 | 0.368085 | 0.3679 | 0.343345875 |
| 57.5 | 4200 | 1.5 | 0.381037 | 0.3781 | 0.343345875 |
| 57.5 | 3600 | 1 | 0.343726 | 0.3413 | 0.310720875 |
| 57.5 | 3600 | 1 | 0.345261 | 0.3413 | 0.310720875 |
| 57.5 | 3600 | 1 | 0.342143 | 0.3413 | 0.310720875 |

### 2.3 Response Surface Methodology

RSM is a collection of statistical and mathematical techniques useful for modelling and analysing problems where a response of interest is influenced by multiple variables. In this study, RSM was employed to develop a second-order polynomial model that describes the relationship between the independent variables—$T$, $V$ and $t$—and the response variable, $MR$.

The general form of the quadratic model used is given as,

$$MR = \beta_0 + \sum_{i=1}^{3}\beta_i X_i + \sum_{i=1}^{3}\beta_{ii} X_i^2 + \sum_{i=1}^{2}\sum_{j=i+1}^{3}\beta_{ij} X_i X_j + \epsilon \quad (2)$$

where $\beta_0$ is the intercept term, $\beta_i$ are the linear coefficients, $\beta_{ii}$ are the quadratic coefficients, $\beta_{ij}$ are the interaction coefficients and $\epsilon$ represents the residual error.

The coefficients were estimated using the method of least squares and the adequacy of the model was evaluated through analysis of variance (ANOVA). Statistical significance was determined at a 95% confidence level.

### 2.4 Genetic Programming

GP is an evolutionary algorithm-based methodology inspired by biological evolution to find computer programs that perform a user-defined task. In this study, GP was

utilized to develop a predictive model for the moisture ratio during the drying of grapes.

*Fig. 3: Dryer tray assembly*

The GP algorithm begins with a randomly generated population of mathematical expressions composed of functions (in this case, addition, subtraction, multiplication, division) and terminals (input variables and constants). The fitness of each expression is evaluated based on its ability to predict the experimental moisture ratio data. The fitness function used was the mean square error (MSE) between the predicted and observed values.

Genetic operators such as selection, crossover and mutation were applied to evolve the population over successive generations. Selection favoured expressions with lower MSE, while crossover and mutation introduced new structures and variations. To prevent overfitting and ensure model interpretability, constraints were imposed on the maximum tree depth and length. The GP-generated model can be expressed as an explicit mathematical equation, providing transparency and ease of interpretation compared to traditional "black-box" ML models.

## 3 RESULTS AND DISCUSSION

### 3.1 Experimental Analysis

Table 2 shows the 15 experiments carried out at various parametric combinations as ascertained by BBD pattern. Primarily, it is observed that drying temperature and time significantly impact moisture ratio, while airflow rate has a moderate effect. Variables such as temperature-time interactions, may also have significant influence. To further understand this, predictive models built using RSM and GP are studied in detail in the subsequent sections.

### 3.2 Development of RSM model

For the RSM model initially a full second-order model is built on which then ANOVA is applied. The insignificant terms in the full second-order RSM model are then identified as those having $p > 0.1$ and are eliminated using stepwise elimination method. The ANOVA for the final RSM model is shown in Table 3. The developed model is of the following form,

$$MR = 0.13796 + 0.000872T + 0.000064t + 0.006351V + 0.000018tV - 0.0000000115t^2 \quad (3)$$

The model itself is highly significant with $F-value$ of 121.23 and $p-values$ less than 0.0001. It is important to note here that the first-order term $t$ in the model has p-value>0.1 but still is not eliminated to maintain hierarchical model.

*Tab. 3: ANOVA results for RSM*

| Source | SS | df | MS | $F-value$ | $p-value$ |
|---|---|---|---|---|---|
| Model | 0.0108 | 5 | 0.0022 | 121.23 | < 0.0001 |
| $T$ | 0.0003 | 1 | 0.0003 | 19.2 | 0.0014 |
| $t$ | 9.34E-07 | 1 | 9.34E-07 | 0.0524 | 0.8235 |
| $V$ | 0.0103 | 1 | 0.0103 | 576.43 | < 0.0001 |
| $tV$ | 0.0001 | 1 | 0.0001 | 6.65 | 0.0275 |
| $t^2$ | 0.0001 | 1 | 0.0001 | 3.84 | 0.0785 |
| Residual | 0.0002 | 10 | 0 | | |
| Lack of Fit | 0.0001 | 7 | 0 | 0.6181 | 0.7302 |
| Pure Error | 0.0001 | 3 | 0 | | |
| Cor Total | 0.011 | 15 | | | |

### 3.3 Development of GP model

Similarly, the GP model is developed using the experimental data and is of the following form,

$$MR = 0.19266 + 0.00091845T + 0.06525V \quad (4)$$

For the GP model, maximum model depth and length is set to 8 and 18 respectively, while the iteration limit is 50 generations. Mean squared error (MSE) is considered as the loss function. As the generations evolve, the relative frequency of the terminals and functions are continuously updated to try and lower the MSE. Figure 4a shows the variation of the terminals and functions across iterations. It is observed that all the functions (i.e., +, -, * and /) start with the same frequency at the start of the training cycle but undergo dynamic changes depending on the fitted GP models. Similarly, in Figure 4b the relative frequency of variables shows a lot of variation. $t$ is observed to be insignificant as its relative frequency is observed to be very close to 0 during the entire training stage. It should be noted here that the GP model shown in equation (4) is simplified version of the actual GP model achieved after the training process.

Figure 5 shows the convergence of GP training process. It shows gradual improvement in average fitness, especially in the early iterations, before levelling off. On the other hand, global fitness (best-performing individual so far) largely remains relatively constant, indicating a high-performing solution early in the process that remains optimal throughout most of the iterations. This suggests that a strong solution was found early and remained largely unchanged throughout the process. This indicates that the GP algorithm quickly identifies an optimal or near-optimal solution and then focuses on refining the population around that high-performing solution.

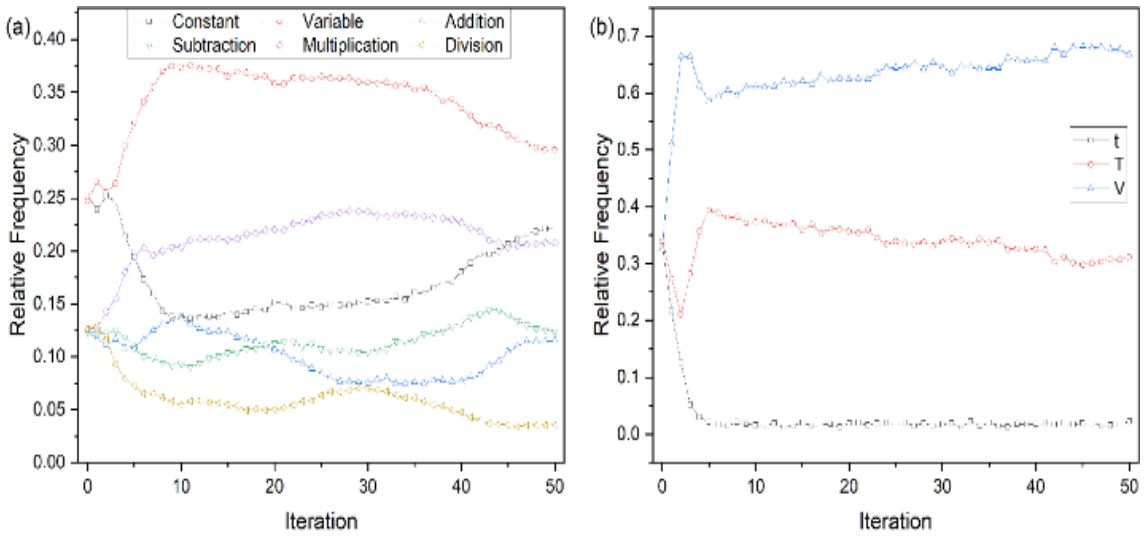


*Fig. 4: Relative frequency across iterations of (a) terminals and functions (b) variables in GP model*

### 3.4 Comparative analysis of RSM and GP

Figure 6 presents the comparative analysis of experimental and predicted values of $MR$ using RSM and GP models. A strong correlation between experimental and predicted values is indicated which means that both the models are quite accurate. The RSM model demonstrates exceptional predictive accuracy, with predicted values closely aligning with experimental values (R = 0.992). The GP model also shows good predictive performance, although slightly lower than RSM (R = 0.983).

The RSM model (Figure 7a) exhibits a tight residual distribution around zero, with residuals ranging from -0.008 to 0.008, indicating high accuracy and precision. The GP model (Figure 7b) shows a wider residual range (0.020 to 0.040), suggesting somewhat less accuracy. Notably, GP residuals are more scattered, particularly at higher

predicted values (0.32-0.40). Figure 8 compares the residuals of both the models against a normal distribution. The data points fall within the expected bounds indicating that the residuals are normally distributed. The mean ($\mu$) and standard deviation ($\sigma$) are shown as $\mu$ = 0.00000625 and $\sigma$ = 0.00346 for RSM and $\mu$ = 0.02848, $\sigma$ = 0.00547 for GP respectively.

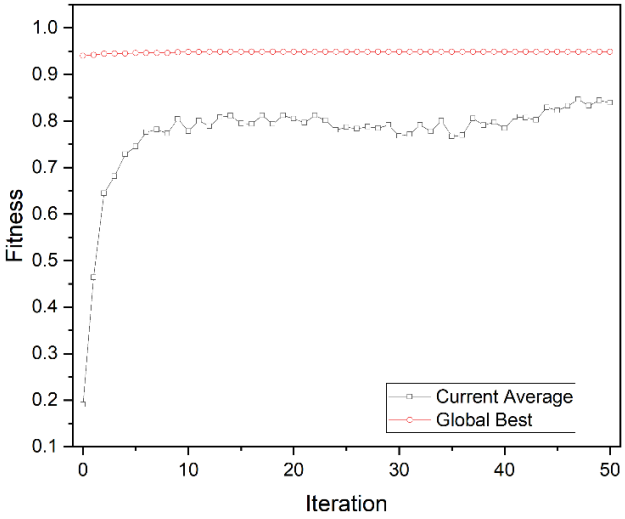


*Fig. 5: Convergence curve of GP*

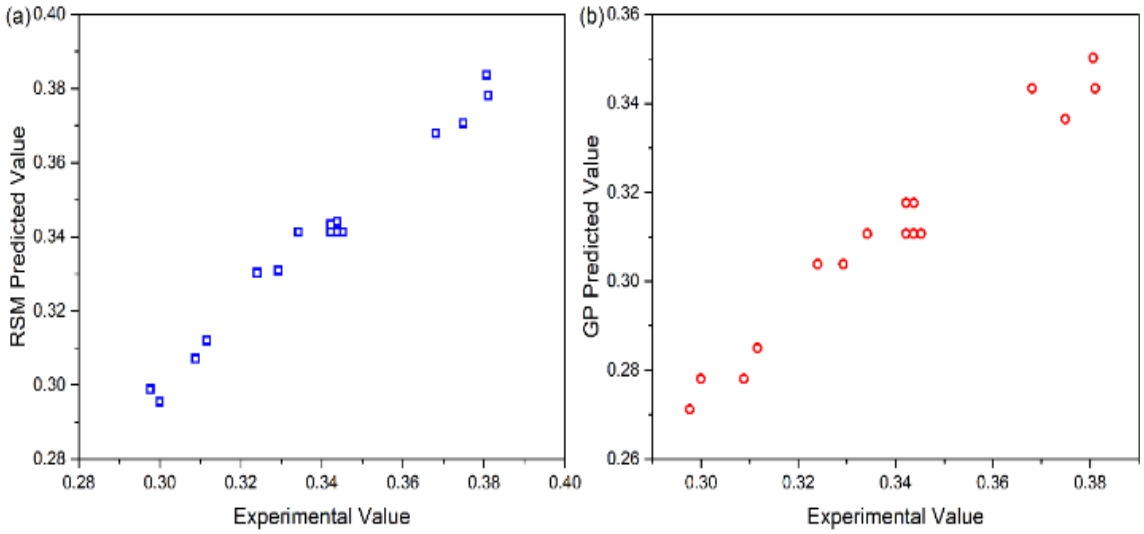


*Fig. 6: Experimental versus predicted value of moisture ratio ($MR$)*

Table 4 indicates that the RSM model, with an R value of 0.992, $R^2$ of 0.984 and Adjusted $R^2$ of 0.973, indicates a high correlation and excellent model fit. However, the complexity of the RSM model, with multiple terms and

higher-order interactions, contrasts with the simplicity of the GP model. Despite the slightly lower accuracy of the GP model, indicated by an R value of 0.983, $R^2$ of 0.966 and Adjusted $R^2$ of 0.957, it still provides a reasonable predictive capability. The Predicted $R^2$ of 0.949 for GP is comparable to the RSM model's 0.953, showing that GP remains effective in predicting new observations. Although the GP model's MSE (0.000839) and MAE (0.028482) are higher, suggesting greater prediction error, the compactness of the GP model offers a clear trade-off.

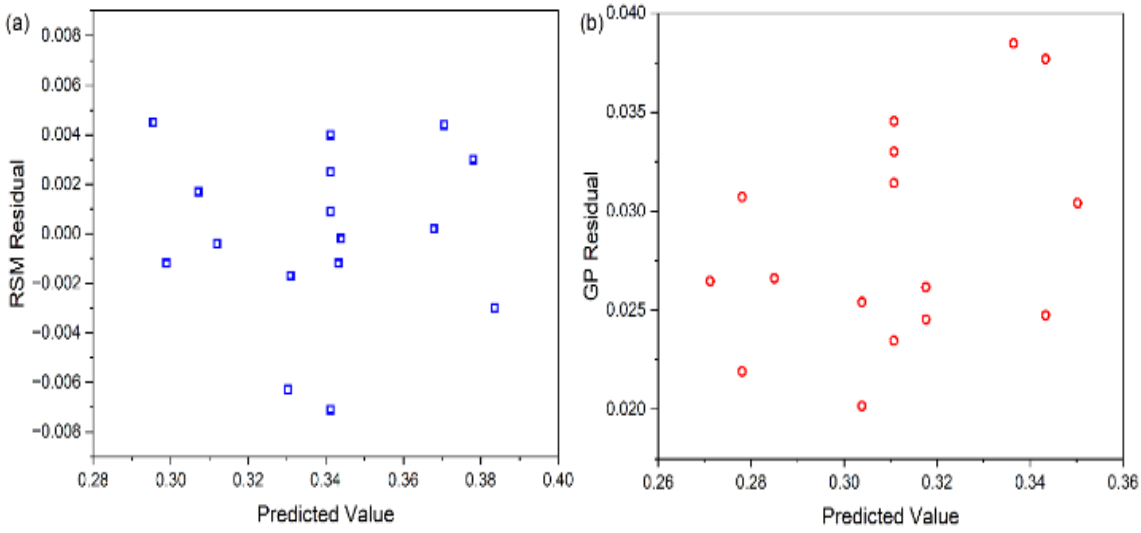


*Fig. 7: Predicted value versus residual of (a) RSM model (b) GP model*

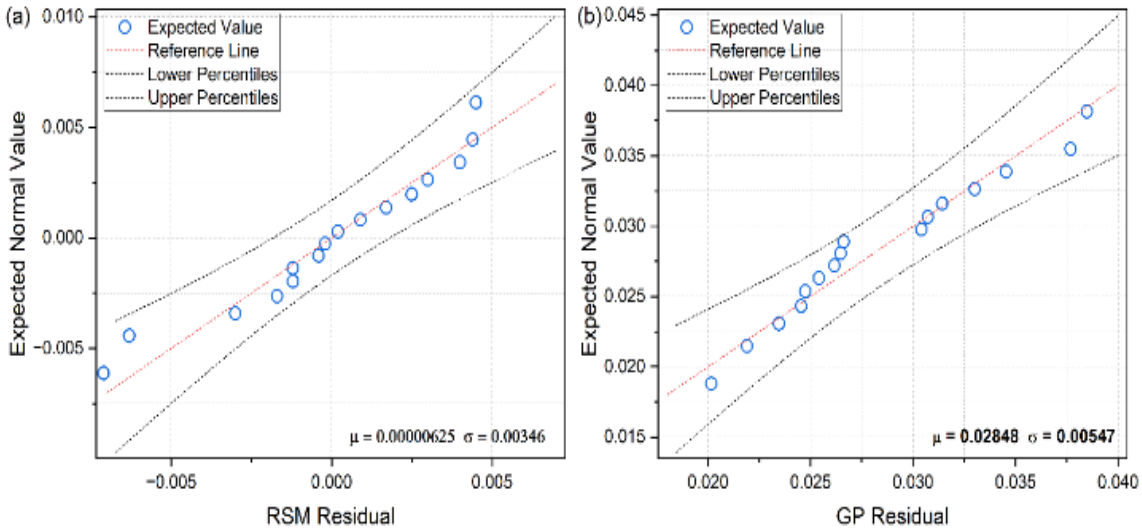


*Fig. 8: Normal probability plot of residual of (a) RSM model (b) GP model*

*Tab. 4: Comparison of prediction performance of RSM and GP model*

| Metric | RSM | GP |
|---|---|---|
| $R$ | 0.992 | 0.983 |
| $R^2$ | 0.984 | 0.966 |
| Adjusted $R^2$ | 0.973 | 0.957 |
| Predicted $R^2$ | 0.953 | 0.949 |
| $MSE$ | 0.000011 | 0.000839 |
| $MAE$ | 0.002622 | 0.028482 |

Figure 10 shows the influence of temperature ($T$ in °C) and airflow velocity ($V$ in m/s) on the moisture ratio ($MR$) based on the GP model. Although the GP model aligns with the RSM model in indicating a negative correlation between temperature and moisture ratio, it exhibits a slightly less pronounced response to airflow velocity. This difference suggests that, while GP captures the fundamental relationships, it might prioritize model simplicity over capturing every subtle interaction, making it suitable for applications requiring straightforward interpretations without sacrificing major accuracy

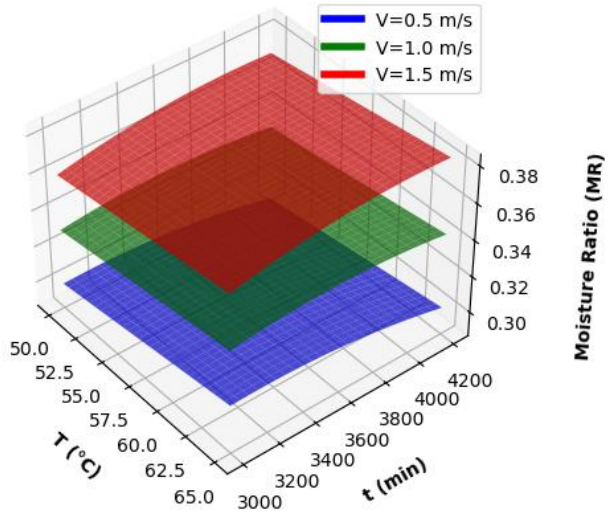


*Fig. 9: Influence of $T$ $(°C)$ and $t$ $(min)$ at various $V$ $(m/s)$ on $MR$ as per RSM model*

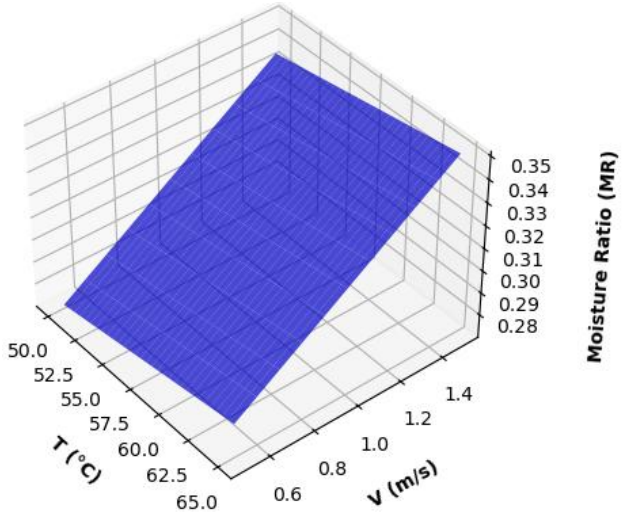


*Fig. 10: Influence of $T$ $(°C)$ and $V$ $(m/s)$ on $MR$ as per GP model*

## 4 CONCLUSION

The study successfully developed and compared predictive models using Response Surface Methodology (RSM) and Genetic Programming (GP) for the moisture ratio in grape drying within a desiccant rotary dryer. Both models demonstrated a strong correlation with experimental data, with RSM achieving slightly higher accuracy than GP. The RSM model, while more complex, provided precise predictions with minimal residuals, whereas the GP model offered a simpler structure with acceptable accuracy, showcasing its utility in applications where model interpretability and compactness are prioritized.

The findings underscore the potential of advanced modeling techniques to optimize drying parameters, which can enhance efficiency in food dehydration processes. Future work could expand on this by exploring hybrid models combining RSM and GP to further improve prediction accuracy and computational efficiency.

## 5 REFERENCES


[Aughenbaugh 2004] henbaugh, J. M., & Paredis, C. J. The role and limitations of modeling and simulation in systems design. Computers and Information in Engineering.2004.

[Baslar 2023] Baslar, M., From fresh to dried: Evaluating drying kinetics of Sultana and Besni grapes. Ipeak. 2023.

[Chen 2023] Chen, C., & Pan, Z. An overview of progress, challenges, needs and trends in mathematical modeling approaches in food drying. Dry. Technol, 2023, 41, 2586-2605.

[Gautam 2024] Gautam, J. K., & Verma, P. Review paper on diffierent types of solar dryer. Int. J. Res. Appl. Sci. Eng. Technol. July 2024, 12, 250-257.

[Homayoonfal 2024] Homayoonfal, M., Malekjani, N., Baeghbali, V., Ansarifar, E., Hedayati, S., & Jafari, S. M. Optimization of spray drying process parameters for the food bioactive ingredients. Crit. Rev. Food Sci. Nutr. 2024, 64, 5631-5671.

[Kalavathidevi 2023] Kalavathidevi, Maheswaran, Sakthivel, Sangavi, Rajaraghavendraa, S., & Kanna, R. Solar powered dryer for drying and storing grapes. 14th International Conference on Computing Communication and Networking Technologies (ICCCNT) 2023. Delhi: IEEE.

[Kilic 2024] Kilic, M., Sahin, M., Hassan, A., & Ullah, A. Preservation of fruits through drying-A comprehensive review of experiments and modeling approaches. J. Food Process Eng. March 2024, 47.

[Lvovich 2019] Lvovich, I. Y., Lvovich, Y. E., Preobrazhenskiy, A. P., Preobrazhenskiy, Y. P., & Choporov, O. N. Modelling of information systems with increased efficiency with application of optimization-expert evaluation. J. Phys. Conf. Ser. December 2019, 1399, 033079.

[Mercer 2024] Mercer, D. G. Concepts of dehydration and drying for small-scale food processors. Royal Society of Chemistry, August 2024.

[Mujumdar 2020] Mujumdar, A. S., & Menon, A. S. Drying of solids: Principles, classification and selection of dryers. In Handbook of Industrial Drying (pp. 1-39). CRC Press, September 2020.

[Nursani 2021] Nursani, D., Hafitara, H., Bagawanta, B., & Surjosatyo, A. Investigation of rotary dryer performance fueled with wood pellets for biomass processing. IOP Conf. Ser. Earth Environ. Sci. May 2021, 749, 012050.

[Palacios Rosas 2023] Palacios Rosas, E., Reyes, A.., Castro-Olivera, P.-M., Acosta-Nava, K.., Vega-Goitia, M., & Palacios, A. Food Drying: Opportunities, Market Solutions and Nutraceutical Properties of Chayote. Alimentos Ciencia E Ingeniería, 2023, 30(2), 1-21.

[Palacios Rosas 2023] Palacios Rosas, E., Reyes, A.., Castro-Olivera, P.-M., Acosta-Nava, K.., Vega-Goitia,

M., & Palacios, A. Food Drying: Opportunities, Market Solutions and Nutraceutical Properties of Chayote. Alimentos Ciencia E Ingeniería, 2023, 30(2), 1-21.

[Singh 2024] Singh, A. P., Gupta, A., Biswas, A., & Das, B. Experimental study of a novel photovoltaic-thermal-thermoelectric generator-based solar dryer for grapes drying. Int. J. Green Energy, April 2024, 21, 1161-1173.

[Ünal 2023] Ünal, M. S., Güler, E., & Yaman, M. Changes in antioxidant and color properties of raisins according to variety and drying method. Horticulturae, July 2023, 9, 771.

[Veeranan 2024] Veeranan, K., Pandian, V., Thamaraiselvi, & Martin, A. Impact of mathematical models in IT system design and optimization. International Journal of Information Technology, Research and Applications, February, 2024, 3, 1-11.

[Yang 2013] Yang, X.-S., Koziel, S., & Leifsson, L. Computational optimization, modelling and simulation: Recent trends and challenges. Procedia Comput. Sci. 2013, 18, 855-860.

[Zhou 2022] Zhou, H. Dryers. In Integration and Optimization of Unit Operations, Elsevier.2022, pp. 145-176.